Supplementary Information (SI) for Journal of Materials Chemistry A.
This journal is © The Royal Society of Chemistry 2025

Supporting Information

Multifunctional Hydroxyurea Additive Enhances High Stability and Reversibility of Zinc Anodes

Ruizhe Zhang ‡ [a], Zhiyong Liao ‡[a], Yongbo Fan[b,*], Lixin Song[a], Jiayi Li[a], Zhuo Zhang[a], Peizhi Dong[a], Zexue Lin[a], Ning Yang[a], Qingfeng Zhang[c], Huiqing Fan [a,*]

a State Key Laboratory of Solidification Processing, School of Materials Science and Engineering, Northwestern Polytechnical University, Xi'an 710072, PR China

b Department of Applied Physics, The Hong Kong Polytechnic University, Hung Hom 100872, Hong Kong, PR China

c Hubei Key Laboratory of Micro-Nanoelectronic Materials and Devices, School of Materials Science and Engineering, Hubei University, Wuhan 430062, PR China

‡ *Equal contribution.*

E-mail addresses of corresponding authors: E-mail address: Email: hqfan@nwpu.edu.cn

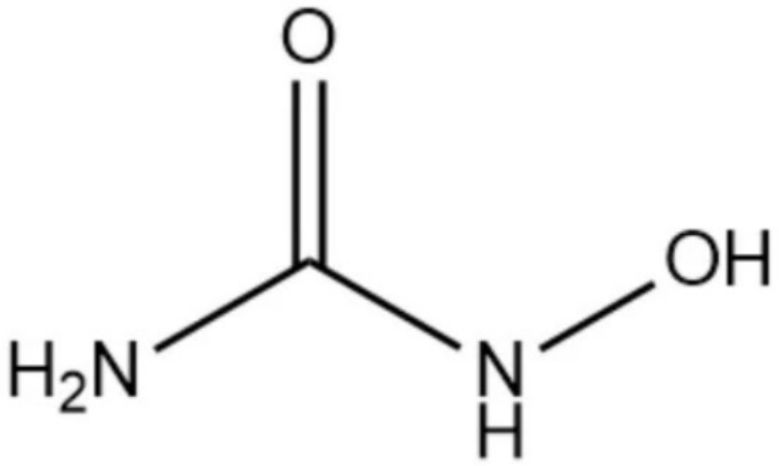

Figure S1. Schematic diagram of hydroxyurea structure.

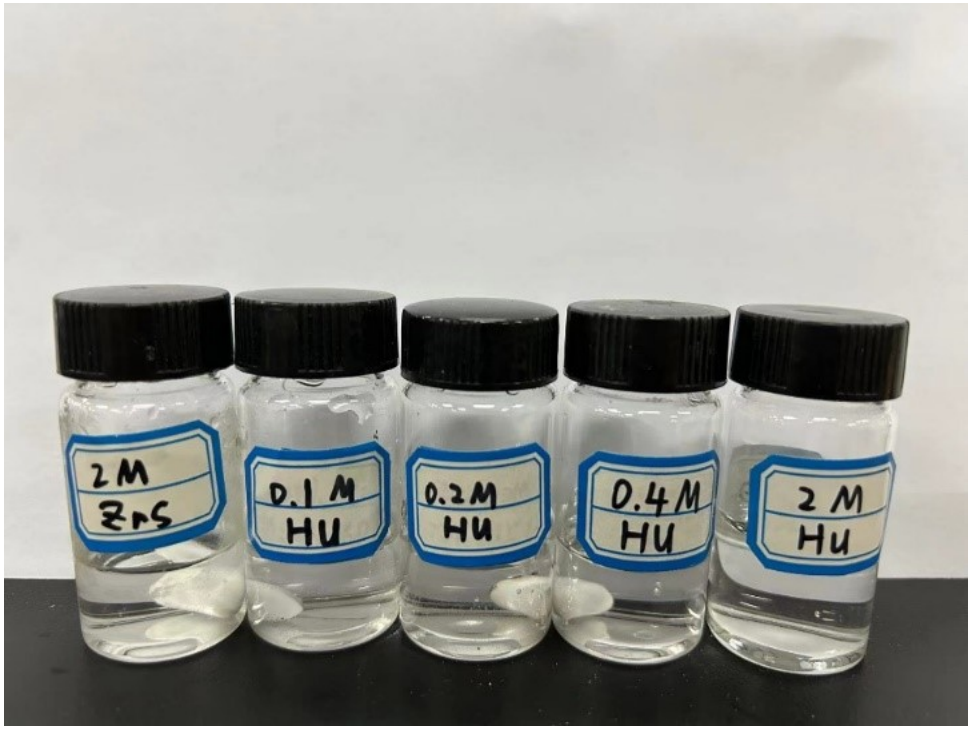

Figure S2. Physical diagram of HU solution with different concentrations.

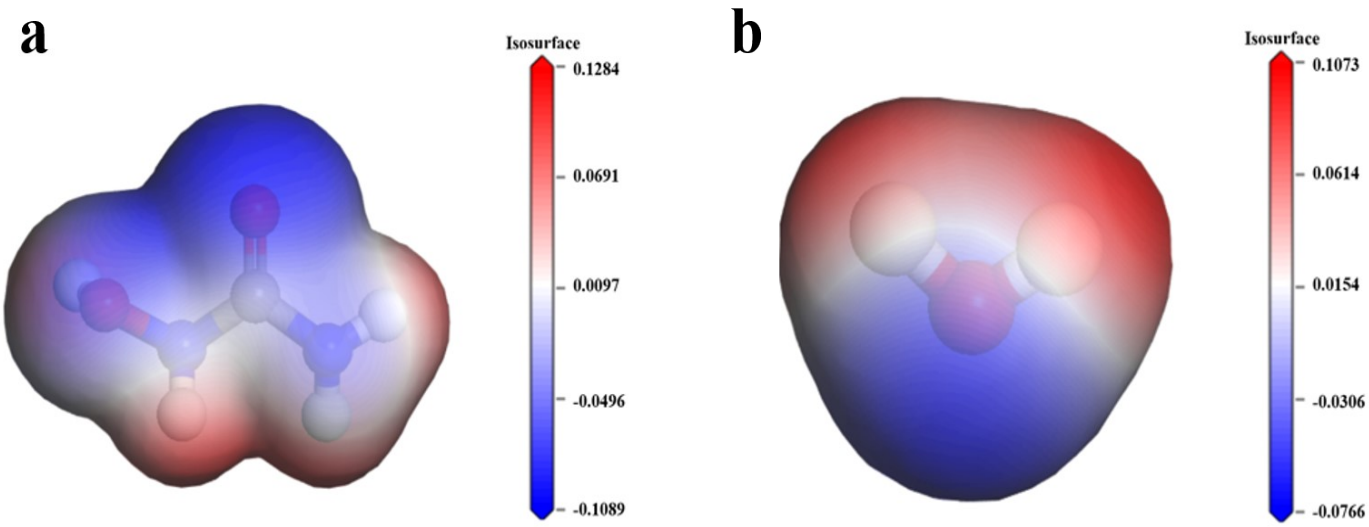

Figure S3. ESP of different molecules: a) HU molecule. b) H_2O molecule.

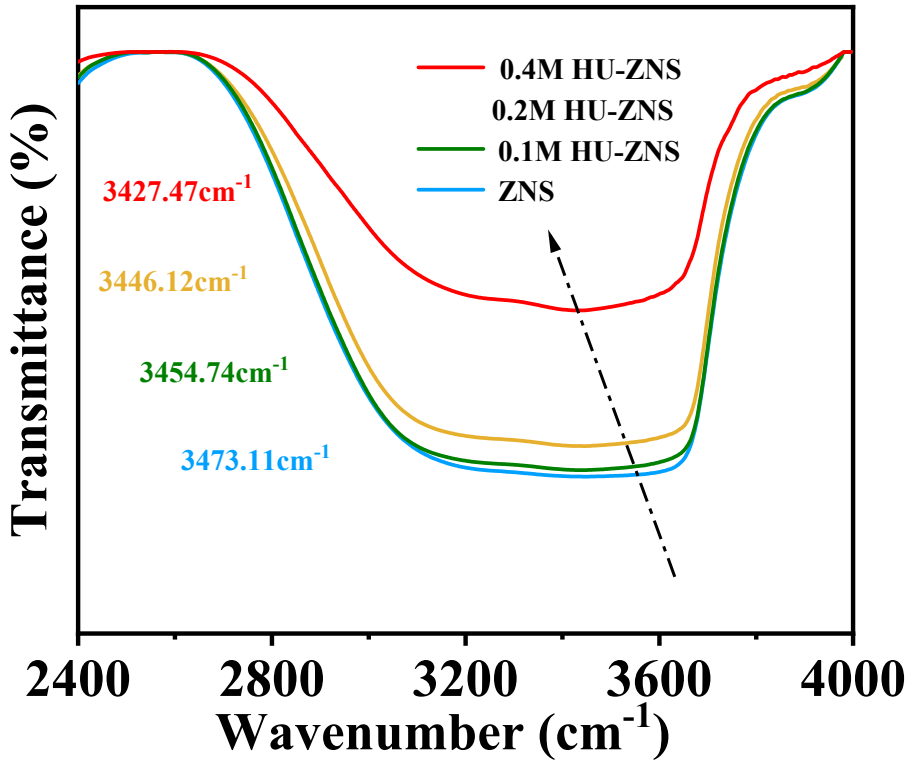

Figure S4. FTIR spectra of O-H bond stretching vibrations for different HU concentrations.

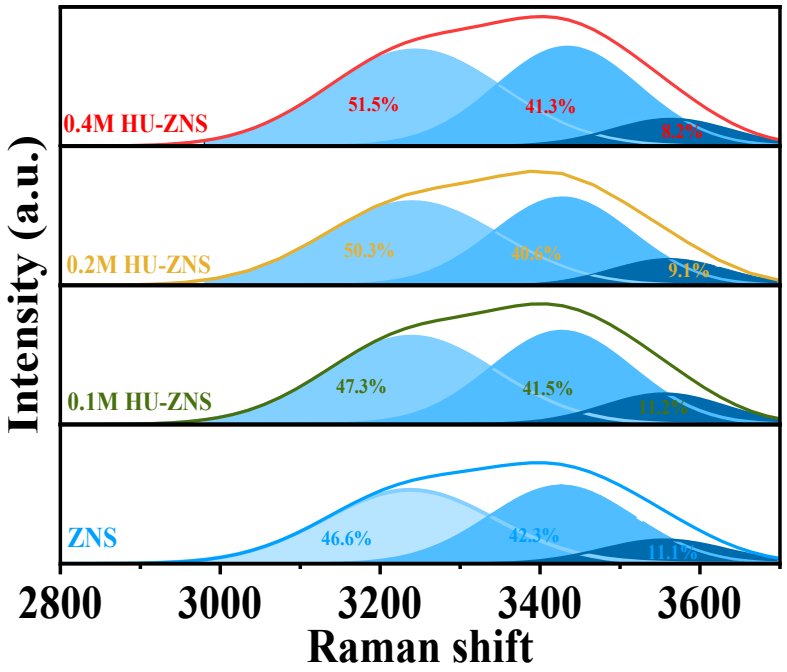

Figure S5. Raman spectra fitted for different HU concentrations.

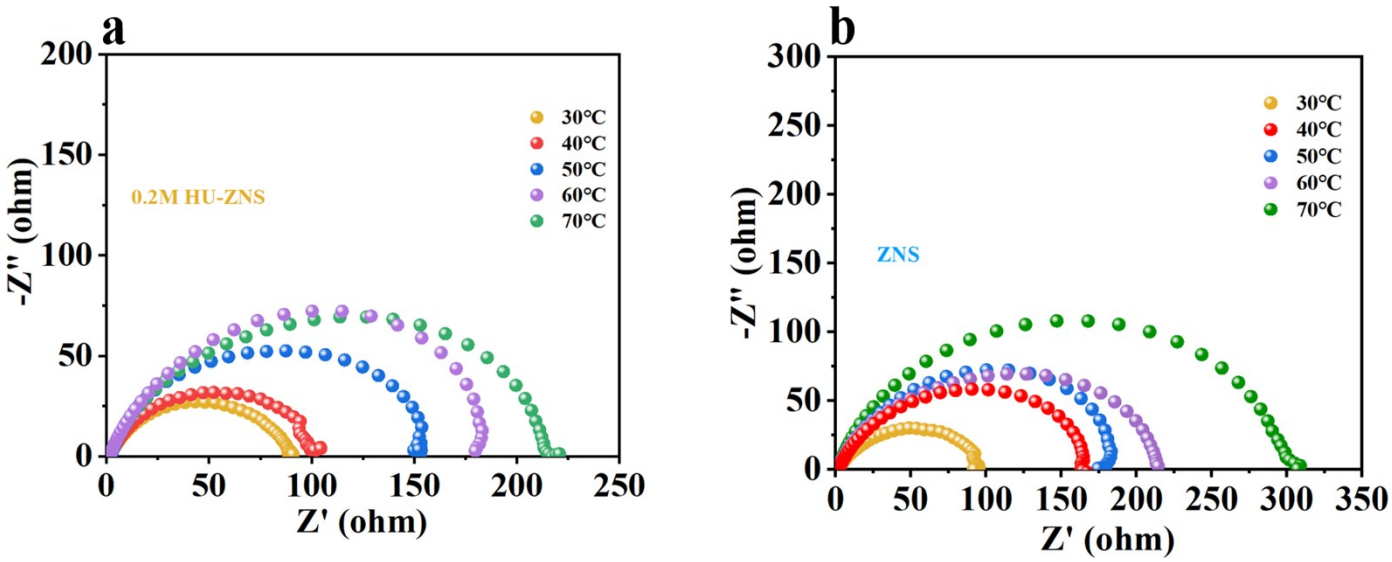

Figure S6. Impedance at different temperatures: a) In 0.2M HU-ZNS electrolyte; b) In ZNS electrolyte.

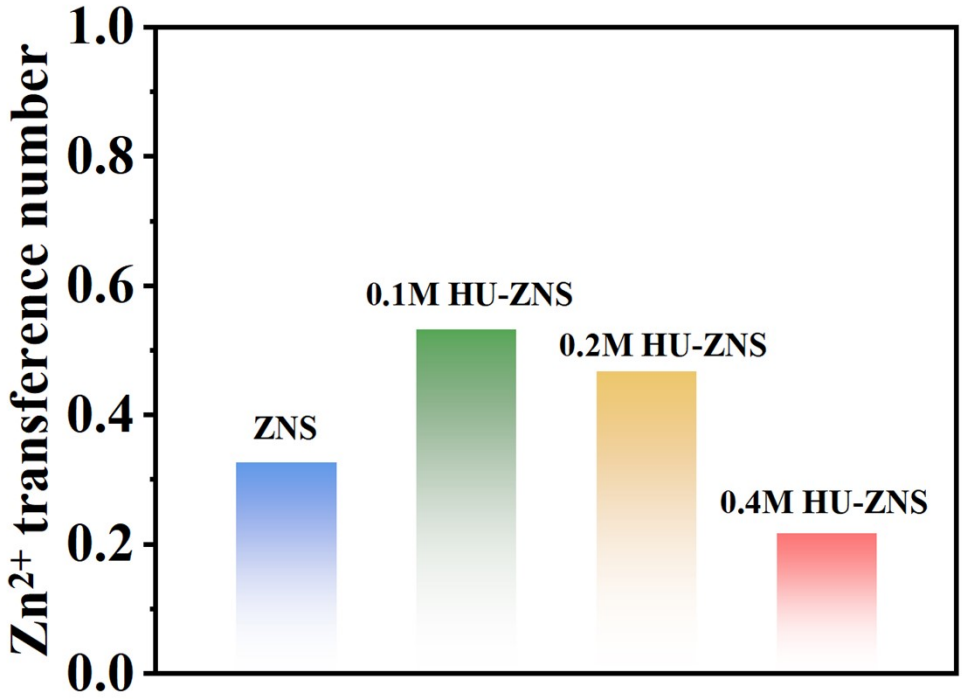

Figure S7. The zinc ion transference number of electrolytes with different concentrations.

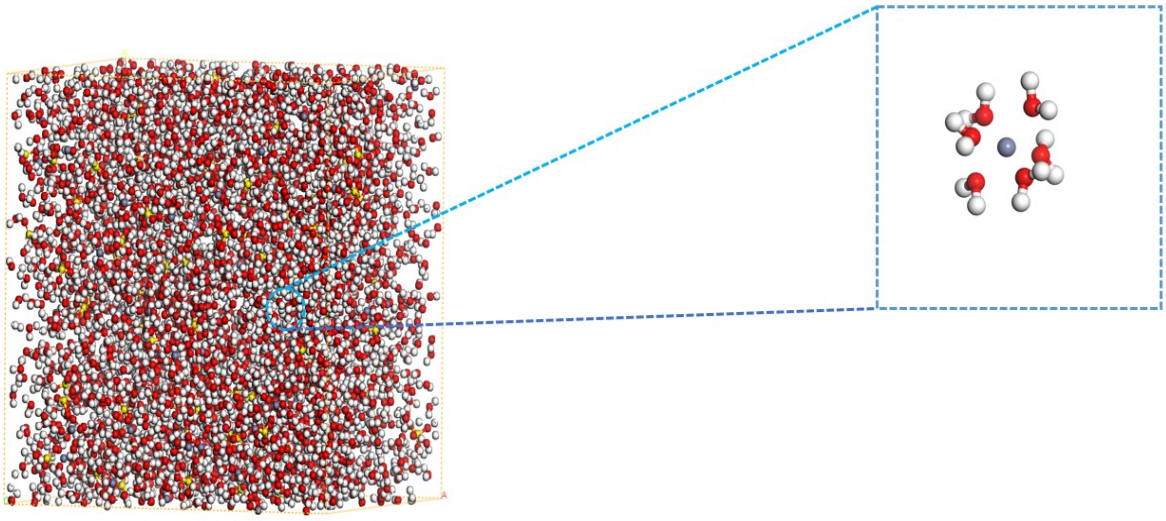

Figure S8. Molecular dynamics simulation of zinc sulfate electrolyte.

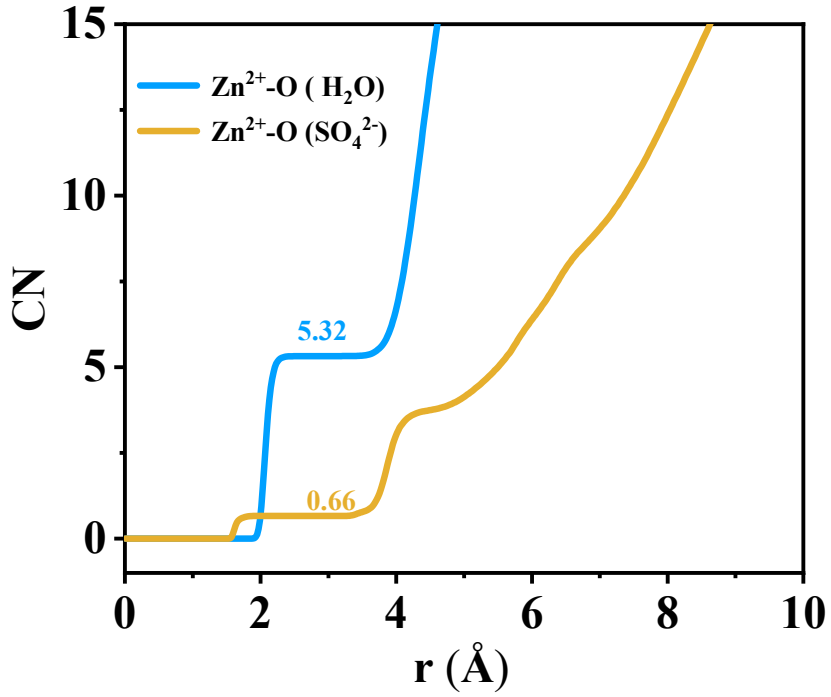

Figure S9. Zn^{2+}-O coordination number function.

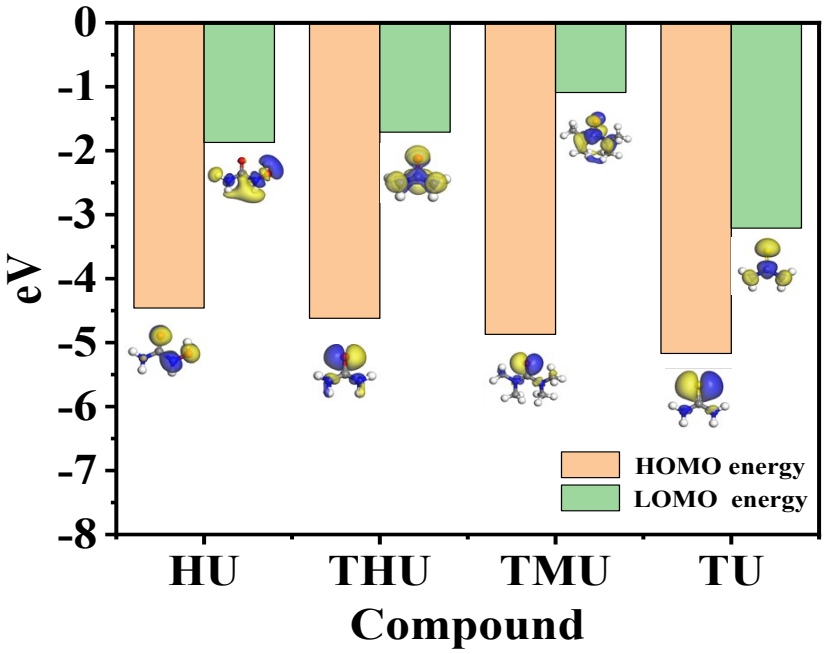

Figure S10. The HOMO and LOMO values of urea-based compounds.

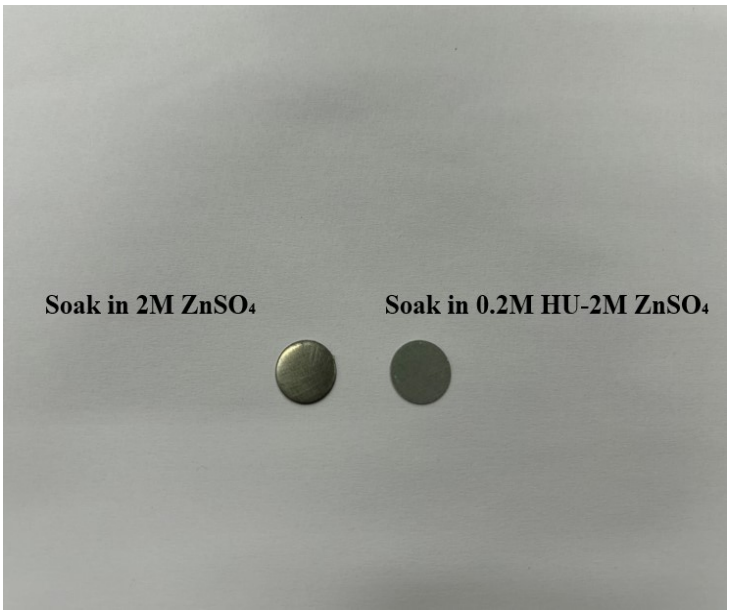

Figure S11. Zn foils soak in different electrolytes.

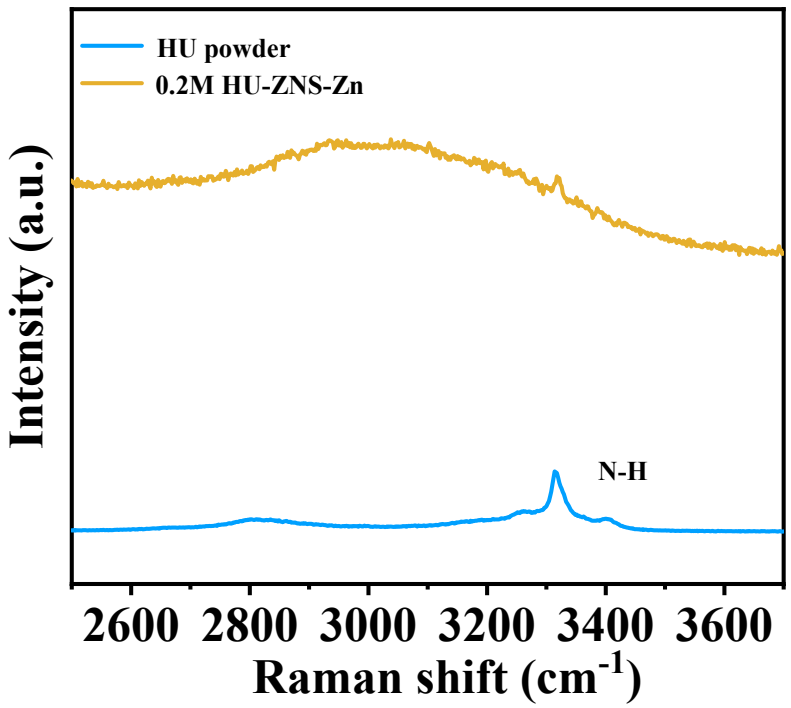

Figure S12. Raman spectrums of pure HU powder and Zn foil (soaked in HU-ZNS electrolyte).

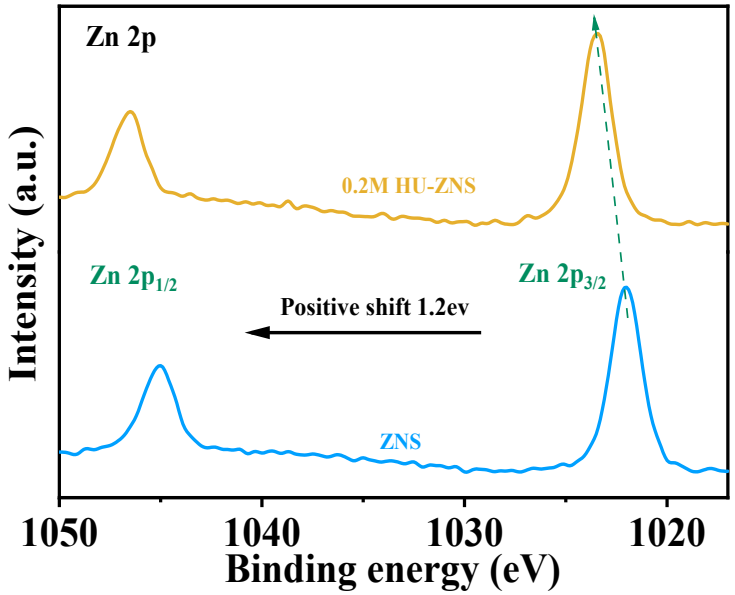

Figure S13. XPS Zn 2p spectra of zinc foil soaked in different electrolytes.

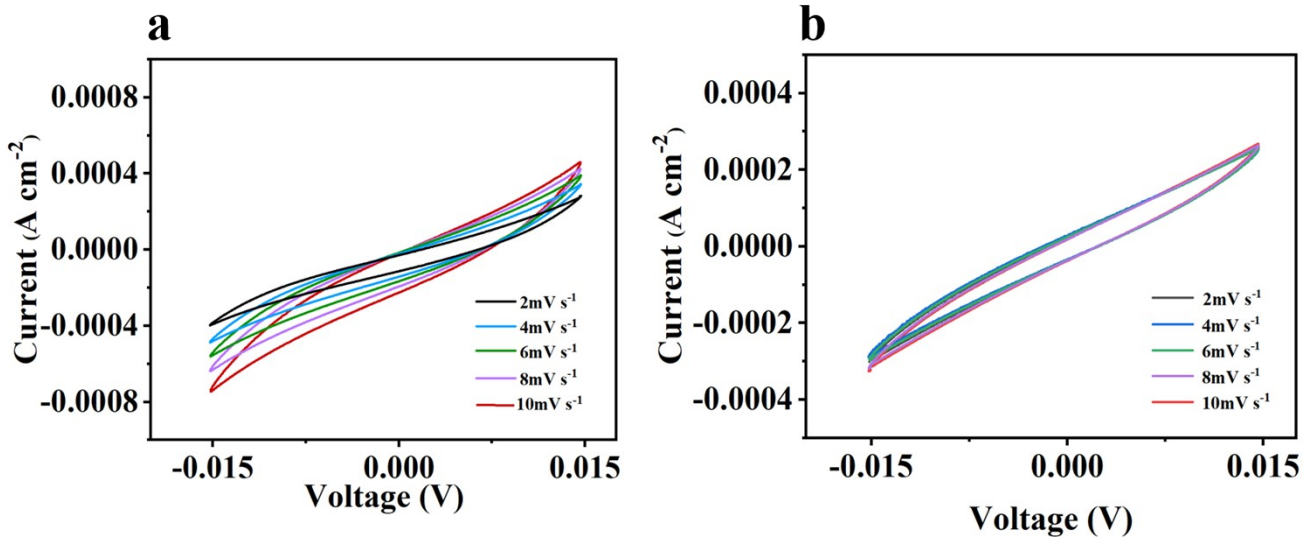

Figure S14. CV curves at different scan rates for different electrolytes: a) In ZNS; b) In 0.2M HU-ZNS.

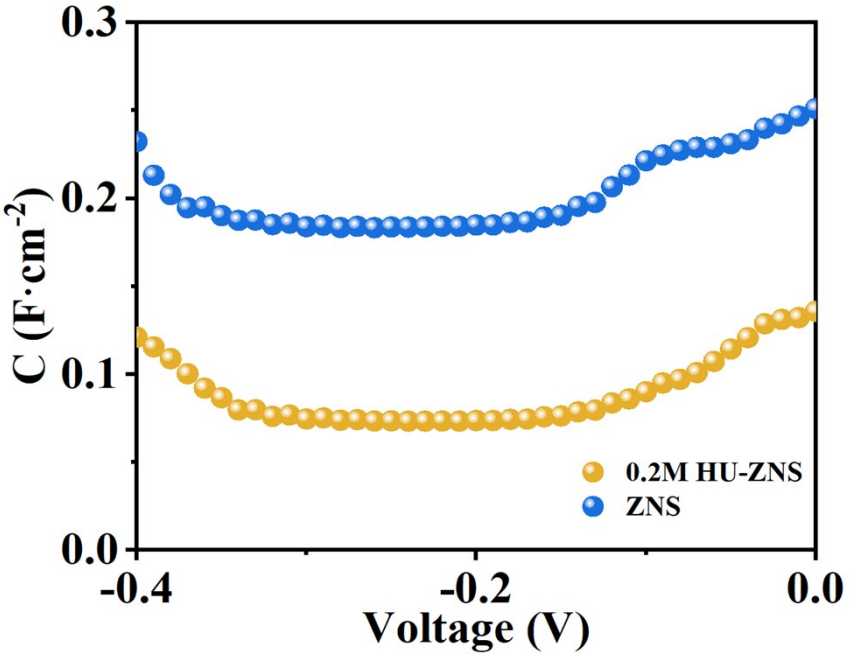

Figure S15. Differential capacitance (DC) curves of different electrolytes.

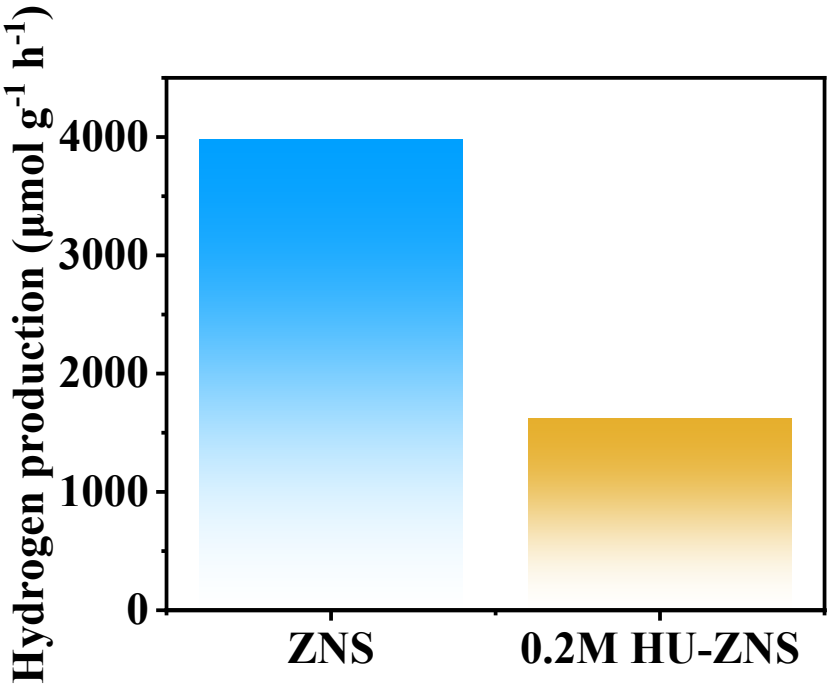

Figure S16. In situ hydrogen evolution rate diagram for different electrolytes.

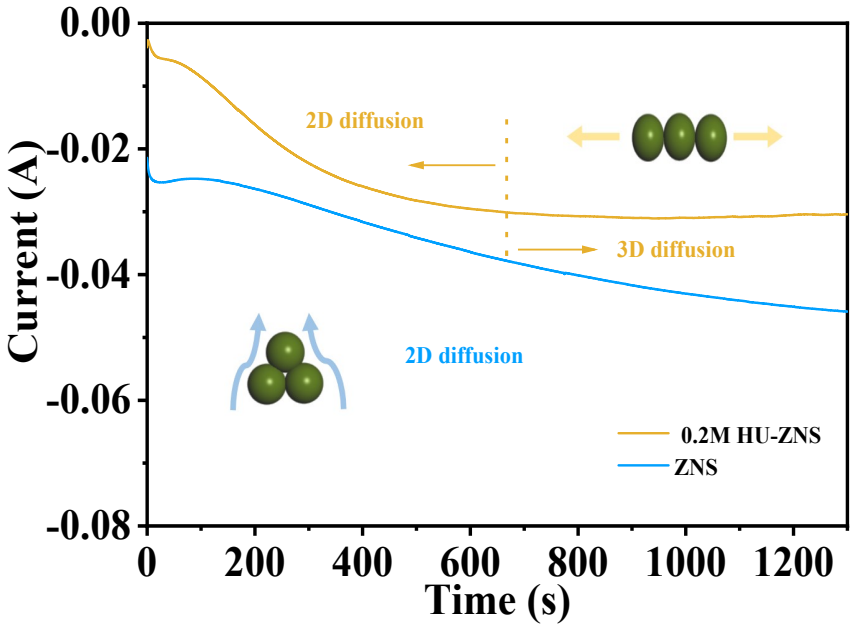

Figure S17. CA curves of different electrolytes.

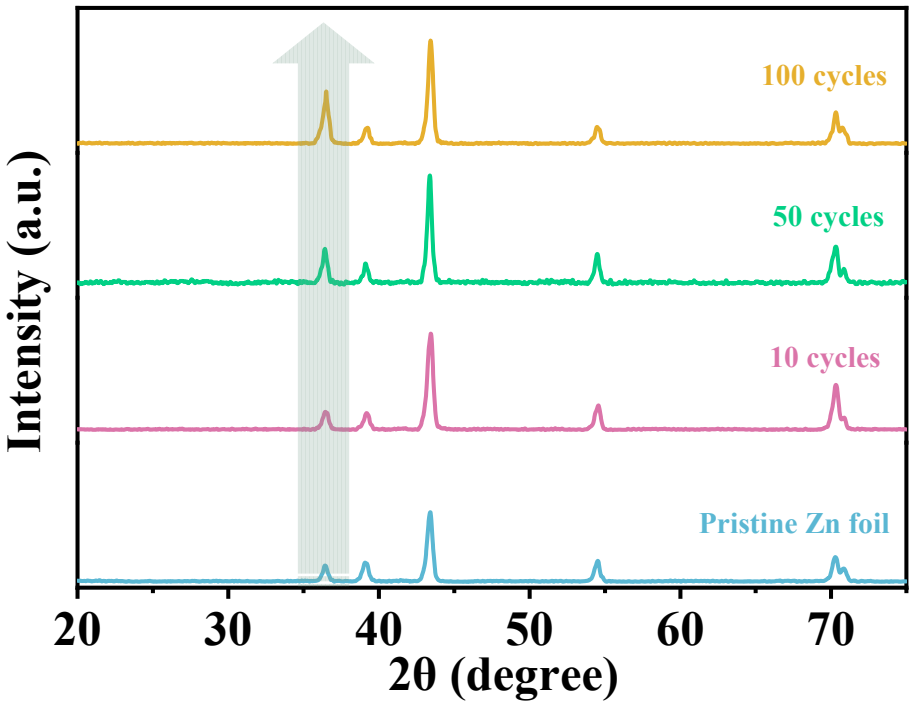

Figure S18. XRD patterns of Zn anodes at different cycle numbers after adding 0.2M HU additives.

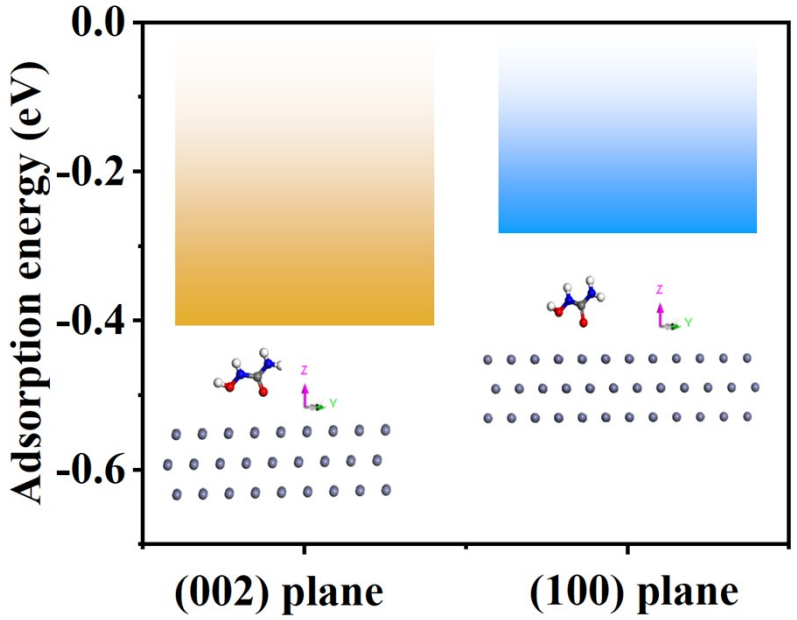

Figure S19. The binding energy of hydroxyurea on different crystal planes.

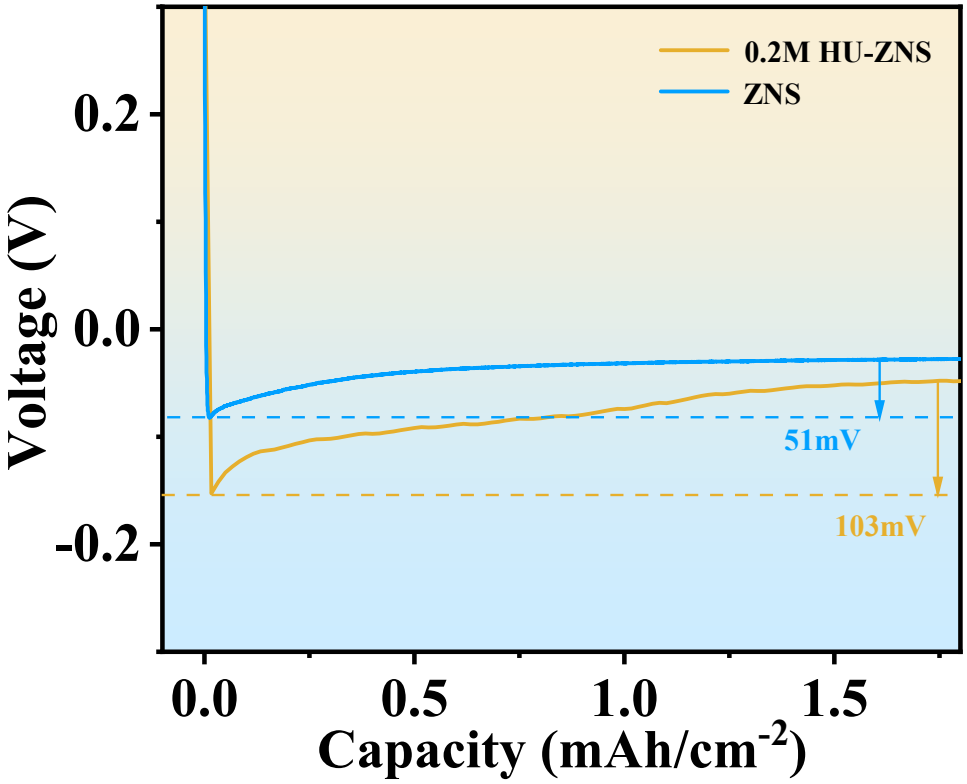

Figure S20. Nucleation potential of Zn//Cu half-cells assembled with different electrolytes.

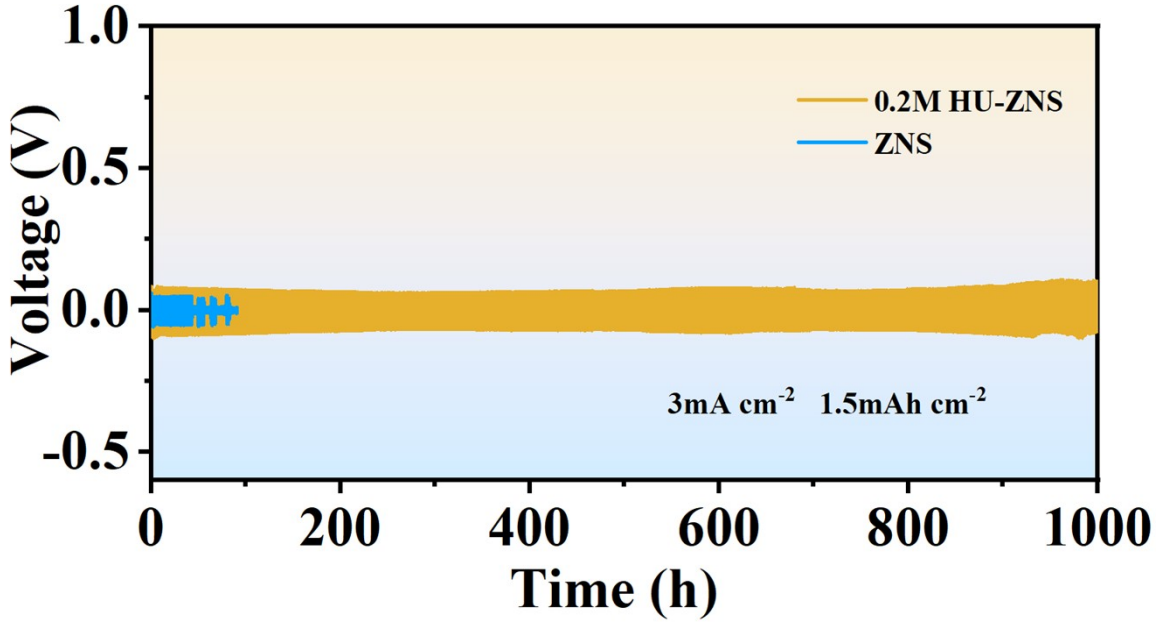

Figure S21. Cycling stability of Zn//Zn symmetric battery at a current density of 3 mA cm^{-2}.

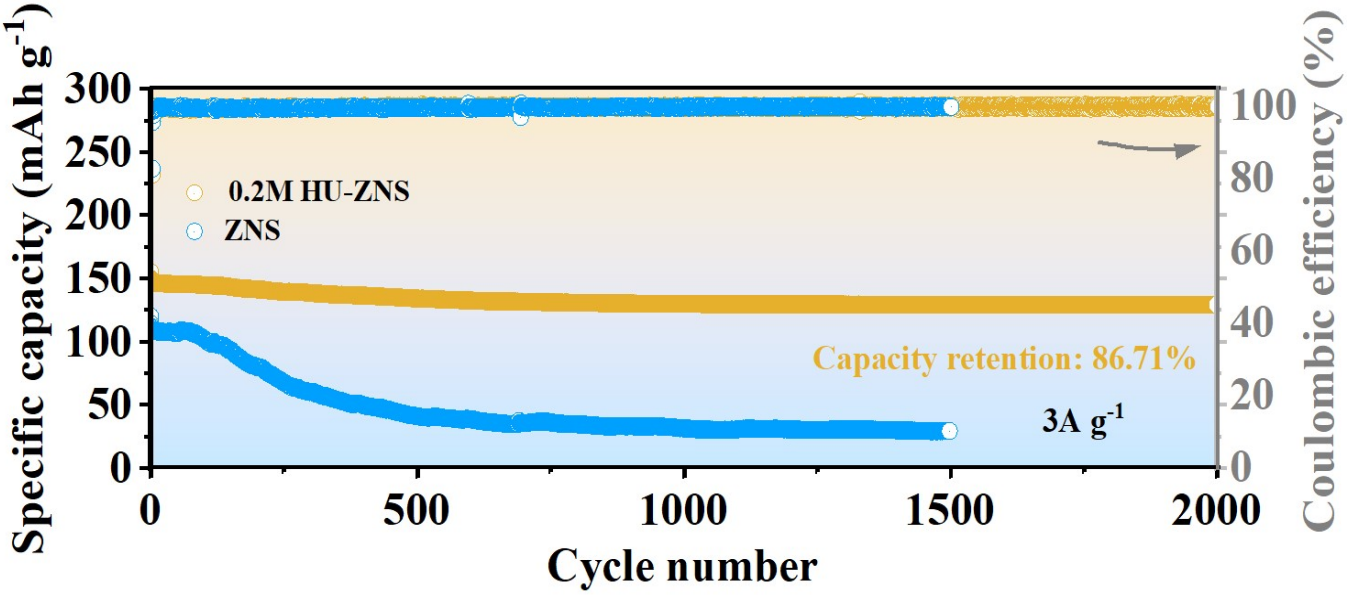

Fig s22. Cycling stability of Zn//MnO_2 coin cell at 3 A g^{-1}.

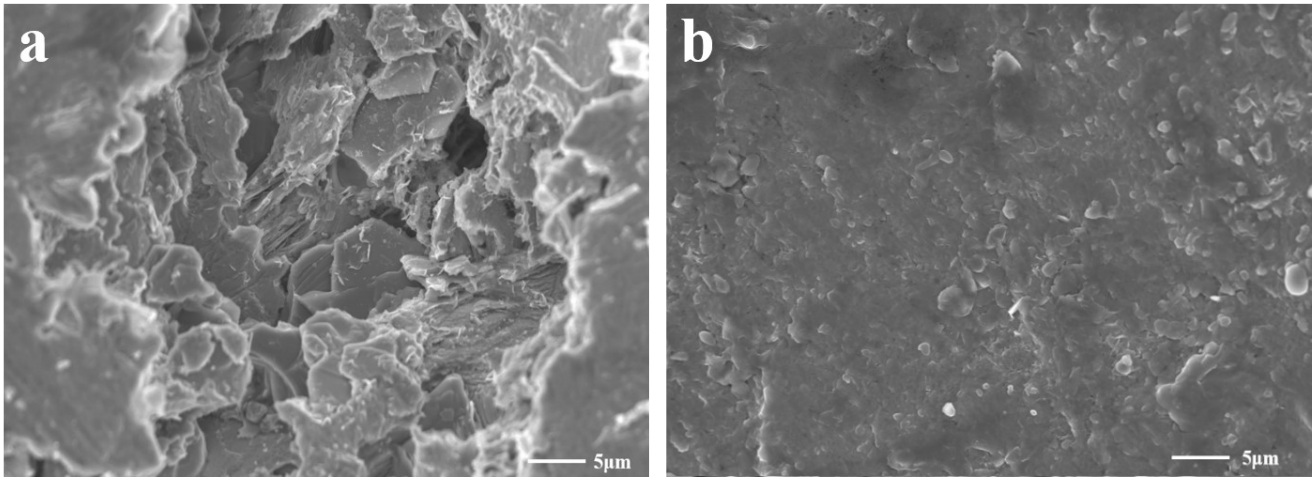

Figure S23. SEM of Zn anode surface morphology after 1400 cycles of Zn//MnO_2 full battery in different electrolytes: a) In ZNS electrolyte; b) In HU-ZNS electrolyte.

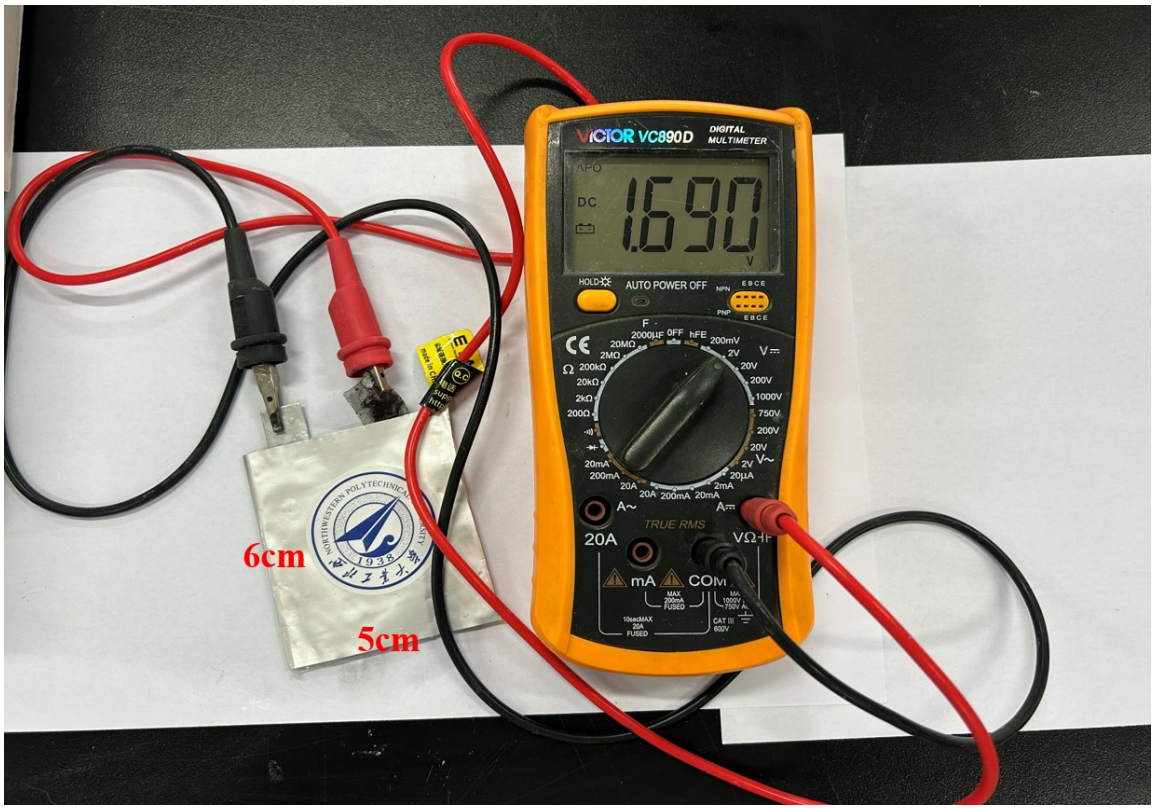

Figure S24. The voltage of Zn//MnO_2 pouch cell.

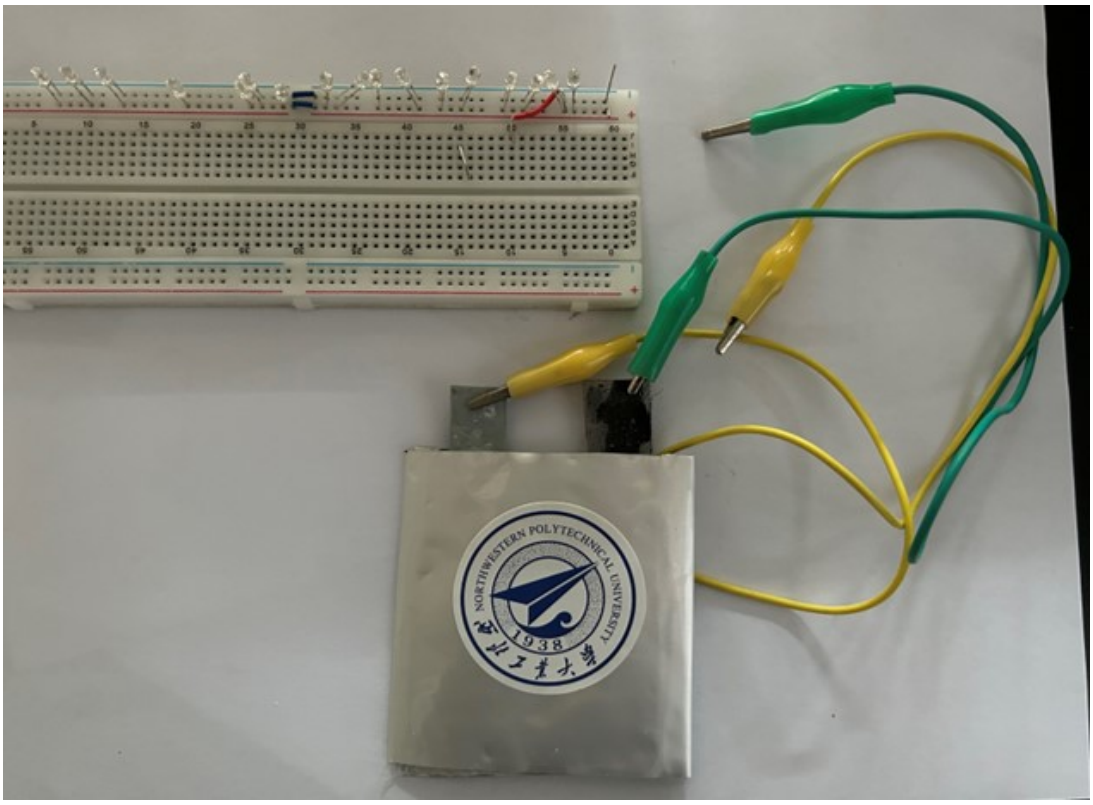

Figure S25. The application as a power source for small lights (not connected to the circuit).